

DL-PDE: Deep-learning based data-driven discovery of partial differential equations from discrete and noisy data

Running Title: Deep-learning based Data-driven PDE Discovery

Hao Xu^a, Haibin Chang^a, and Dongxiao Zhang^{a,b,*}

^a BIC-ESAT, ERE, and SKLTCS, College of Engineering, Peking University, Beijing 100871, China

^b Intelligent Energy Lab, Frontier Research Center, Peng Cheng Laboratory, Shenzhen 518055, China

* Corresponding author.

E-mail address: 390260267@pku.edu.cn (H. Xu); changhaibin@pku.edu.cn (H. Chang); donzhang01@gmail.com (D. Zhang).

Abstract: In recent years, data-driven methods have been utilized to learn dynamical systems and partial differential equations (PDE). However, major challenges remain to be resolved, including learning PDE under noisy data and limited discrete data. To overcome these challenges, in this work, a deep-learning based data-driven method, called DL-PDE, is developed to discover the governing PDEs of underlying physical processes. The DL-PDE method combines deep learning via neural networks and data-driven discovery of PDEs via sparse regressions, such as the least absolute shrinkage and selection operator (Lasso) and sequential threshold ridge regression (STRidge). In this method, derivatives are calculated by automatic differentiation from the deep neural network, and equation form and coefficients are obtained with sparse regressions. The DL-PDE is tested with physical processes, governed by groundwater flow equation, contaminant transport equation, Burgers equation and Korteweg–de Vries (KdV) equation, for proof-of-concept and applications in real-world engineering settings. The proposed DL-PDE achieves satisfactory results when data are discrete and noisy.

Keywords: data-driven discovery; machine learning; deep neural network; sparse regression; noisy data.

1. Introduction

As data acquisition and storage ability have increased, data-driven methods have been used for solving various problems in different fields. In recent years, data-driven discovery of governing equations of physical problems has attracted much attention and been investigated in numerous works. Among these investigations, sparse regression methods are frequently utilized techniques, which show promising behaviors for discovering the governing equations of various problems. Using sparse regression aims to identify a small number of terms that constitute a governing equation from a predefined large candidate library, and a parsimonious model can usually be obtained. Brunton et al. (2016) proposed a framework of sparse identification of nonlinear dynamics (SINDy). Rudy et al. (2017) utilized the sequential threshold ridge regression (STRidge) to discover partial differential equations (PDE) from data. Schaeffer (2017) employed the L^1 regularized least-

squares (Lasso) to identify PDE from data. Since then, a large body of extant literature has investigated data-driven discovery of governing equations using sparse regression, for example, discovery of dynamical systems using information criteria (Mangan et al., 2017), identification of dynamical systems and bifurcation using group sparsity (Schaeffer et al., 2017), sparse model selection via integral terms (Schaeffer & McCalla, 2017), discovery of stochastic dynamical equations (Boninsegna et al., 2018), identification of nonlinear dynamics with abrupt system changes (Quade et al., 2018), discovery of high-dimensional dynamics from limited data (Schaeffer et al., 2018), identification of nonlinear dynamics with model predictive control (Kaiser et al., 2018), discovery of governing physical laws using threshold sparse Bayesian regression (Zhang & Lin, 2018), convergence analysis of the SINDy (Zhang & Schaeffer, 2019), discovery of parametric PDE (Rudy et al., 2019), identification of PDEs in complex datasets (Berg & Nyström, 2019), discovery of coordinates and governing equations (Champion et al., 2019), identification of multiscale model for materials (Brunton & Kutz, 2019), discovery of subsurface flow equations (Chang & Zhang, 2019a), and identification of physical processes via a combined data-driven and data-assimilation method (Chang & Zhang, 2019b). Despite the numerous successes achieved with sparse regression-based methods, major challenges remain when faced with noisy data and limited data. Since numerical approximation of derivatives is requisite in these methods, the results may be unstable and ill-conditioned when handling noisy data (Baydin et al., 2018). Brunton et al. (2016) utilized the total variation regularized derivative dealing with noisy data. Rudy et al. (2017) used polynomial interpolation for calculating derivatives from noisy data. Schaeffer and McCalla (2017) proposed to employ the integral form of the differential equation for handling noisy data. However, these strategies can only lessen the difficulties associated with noisy data to a certain extent.

Besides the sparse regression method, other techniques, such as Gaussian process and neural networks, are also utilized for performing data-driven discovery of governing equations. For example, Raissi et al. (2017) and Raissi and Karniadakis (2018) proposed a framework that utilizes the Gaussian process to discover governing equations. In their proposed framework, the parameters of the differential operator are turned into hyper-parameters of some covariance functions, and are learned by the maximum likelihood method. Raissi et al. (2019) proposed a physics-informed neural networks (PINN) for solving forward and inverse problems of PDE. In the PINN, by adding a PDE constraint term in the loss function besides the data match term, the accuracy of the results can be improved, and the coefficients of the PDE terms can be learned. Further works regarding the PINN, among many others, can be found in Yang et al. (2018), Pang et al. (2018), Zhang et al. (2019), and Lu et al. (2019). Avoiding the numerical approximation of derivatives, both the Gaussian process-based method and the neural network-based method require less data and are less sensitive to data noise. However, in the above-mentioned works, the PDE of a considered problem is supposed to have a known structure and only the coefficients of the PDE terms are learned from data, which limit its application for PDE discovery. To overcome this limitation, Raissi (2018) modified the PINN by introducing two neural networks for approximating the unknown solution, as well as the unknown PDE. Even though this modification enables the PINN to solve problems with unknown PDE structures, the learned neural network approximation of the unknown PDE exists as a black box, and thus lacks interpretability. A novel method using neural networks for discovering PDE was proposed in Long et al. (2018). In their work, a convolutional neural network is constructed using learnable constrained filters. According to a relationship between the constrained filters and the finite difference approximation of differential operators, the form of the unknown PDE can be

identified. However, parsimony of the results may not be guaranteed.

For discovery of governing equations, a qualified data-driven method should obtain an interpretable, parsimonious model with high accuracy, and it should be insensitive to data noise. Learning from the advantages and disadvantages of the existing methods, in this work, we propose a new data-driven method, called DL-PDE, which combines deep neural network and sparse regression method for discovery of PDE. For a physical problem, a deep neural network is first introduced to approximate its response, which is trained using available data. According to the universal approximation theorem of neural network, functions of any complexity can be approximated by a neural network with any precision (Cybenko, 1989; Hornik et al., 1989). Next, similar to that in sparse regression-based methods, a candidate library of potential PDE terms is designed, which usually comprises some partial derivatives with respect to temporal or spatial variables. Then, automatic differentiation of neural networks can be utilized to easily access the derivatives at any point. Different from numerical differentiation, automatic differentiation offers the advantages of small influence of noise, good stability, and desirable expandability. Furthermore, a large amount of meta-data are generated using the trained neural network, and the candidate library terms are evaluated at these generated meta-data points. Finally, sparse regression methods, such as Lasso, STRidge and sparse Bayesian, are adopted to identify the sparse terms from the candidate library that constitute a PDE. The proposed DL-PDE method inherits the properties of both the neural network method and sparse regression method, and thus can obtain a parsimonious model and can be insensitive to data noise. Four PDEs, including groundwater flow equation, contaminant transport equation, Burgers equation and KdV equation, are utilized for testing the proposed method. The influence of noisy data and limited discrete data are investigated, and satisfactory results are obtained.

2. Methodology

2.1 PDE discovery

In this work, we aim to investigate the data-driven discovery of PDEs with the following form:

$$u_t = \Phi(u) \cdot \xi, \quad (1)$$

with

$$\Phi(u) = [1, u, u^2, u_x, u_{xx}, \dots, uu_x, uu_{xx}, \dots]. \quad (2)$$

where u denotes the solution of the considered problem; $\Phi(u)$ denotes the candidate library of potential PDE terms; and ξ denotes the coefficient vector. In this work, $\Phi(u)$ is supposed to be sufficiently rich, which means that the terms that constitute the PDE of the considered problem are contained in $\Phi(u)$.

Considering that a PDE usually consists of a small number of terms, data-driven discovery of a PDE aims to find a sparse coefficient. In order to learn the coefficient, spatial and temporal observation data are requisite. Here, observation data (or meta-data) are denoted as $\{(x_i, t_i)\}_{i=1}^N$.

Since the PDE holds for each data point, we have:

$$\begin{bmatrix} u_t(x_1, t_1) \\ u_t(x_2, t_2) \\ \vdots \\ u_t(x_N, t_N) \end{bmatrix} = \begin{bmatrix} 1 & u(x_1, t_1) & \cdots & uu_{xx}(x_1, t_1) & \cdots \\ 1 & u(x_2, t_2) & \cdots & uu_{xx}(x_2, t_2) & \cdots \\ \vdots & \vdots & \ddots & \vdots & \ddots \\ 1 & u(x_N, t_N) & \cdots & uu_{xx}(x_N, t_N) & \cdots \end{bmatrix} \cdot \xi, \quad (3)$$

which can be rewritten as:

$$U_t = \Theta(U) \cdot \xi. \quad (4)$$

Here, note that for learning ξ , U_t and $\Theta(U)$ should be prepared beforehand, and $\Theta(U)$ usually contains different orders of derivative of u with respect to the spatial variable at all data points. Thus, calculating the derivatives contained in U_t and $\Theta(U)$ is necessary for learning ξ . Numerical approximation of derivatives from data is straightforward, for example, using the finite difference method. However, the results may be unstable and ill-conditioned when dealing with noisy data (Baydin et al., 2018). In this work, we acquire the derivative values by using automatic differentiation from the neural network approximation, which will be discussed in the following subsection.

2.2 Neural network

In this work, a neural network is utilized to approximate the physical problem solution and obtain the required derivatives in Eq. (4). Here, we first briefly introduce the neural network approximation. A feed forward fully-connected neural network is utilized in this work, and its structure is shown in Fig. 1. The neural network contains an input layer, an output layer, and one or several layer(s) between the input and output layers that are termed hidden layer(s). Each hidden layer is composed of multiple neurons. Two adjacent layers are connected as:

$$\mathbf{z}_l = \sigma(\mathbf{W}_l \mathbf{z}_{l-1} + \mathbf{b}_l), l = 1, \dots, L-1 \quad (5)$$

where l denotes the layer index; \mathbf{W} denotes the weight matrix; \mathbf{b} denotes the bias vector; and σ denotes the activation function. Thus, using a neural network approximation, the relationship between the input vector \mathbf{z}_0 and output prediction \mathbf{z}_L can be expressed as follows:

$$\mathbf{z}_L = NN(\mathbf{z}_0; \theta) = \sigma(\mathbf{W}_L \sigma(\cdots \sigma(W_2 \sigma(W_1 \mathbf{z}_0 + \mathbf{b}_1) + \mathbf{b}_2)) + \mathbf{b}_L), \quad (6)$$

where θ denotes the collection of all learnable coefficients, which can be expressed as:

$$\theta = \{W_1, b_1, W_2, b_2, \dots, W_L, b_L\}. \quad (7)$$

For approximating the solution of a physical problem, the input vector comprises the spatial and temporal variable, which is $\mathbf{z}_0 = [x, t]^T$; the output prediction is a scalar being of $u(x, t)$.

Suppose that there are N observation data, $\{u(x_i, t_i)\}_{i=1}^N$. In order to train the neural network, a loss

function is then defined as:

$$Loss(\theta) = \sum_{i=1}^N [u(x_i, t_i) - NN(x_i, t_i; \theta)]^2. \quad (8)$$

In this work, the Adam optimizer is utilized to minimize the loss function for training the neural network (Kingma et al., 2014).

As discussed in the previous subsection, derivative calculation is always required for data-driven discovery of PDE. After training the neural network, the required derivatives can be easily accessed by applying the automatic derivation (Baydin et al., 2018). Automatic differentiation is achieved by the back propagation characteristics of the neural network. Different from numerical differentiation, automatic differentiation possesses the advantages of small influence of noise, desirable stability, and good expandability. In addition, besides the observation data, a large amount of meta-data can be generated using the trained neural network, which can facilitate the sparse regression to achieve stable results, as detailed in section 3.6.2.

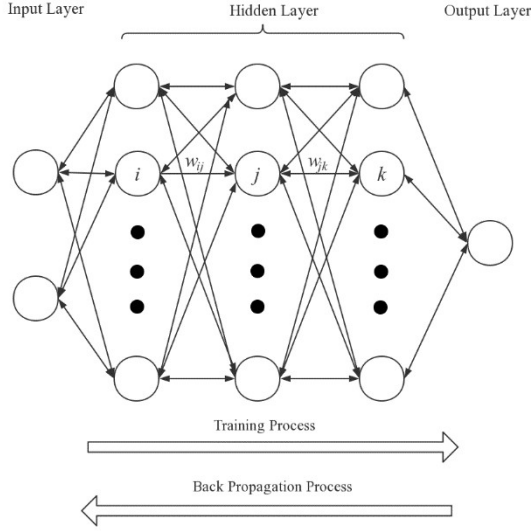


Fig. 1. The structure of a feed forward fully-connected neural network. The forward arrow indicates the training process of the neural network, and the backward arrow indicates the back propagation process of the neural network.

2.3 DL-PDE

In this work, we propose a new data-driven method, called DL-PDE, which combines deep neural network and sparse regression method for discovering PDE. In the DL-PDE, a candidate library for PDE discovery is first designed. Next, a neural network is trained using the observation data to approximate the solution of the considered problem. A large amount of meta-data is then generated using the trained neural network, and the candidate library terms are evaluated at these generated meta-data points. Finally, the sparse regression method is adopted to identify the sparse terms from the candidate library that constitute a PDE. Note that although STRidge (Rudy et al., 2017) is found suitable and hence adopted in this study, other sparse regression methods, such as Lasso (Schaeffer, 2017) and sparse Bayesian inference (Zhang & Lin, 2018), can also be employed for this purpose.

Here, we briefly introduce STRidge, additional details of which can be found in Rudy et al. (2017). Solving Eq. (4) using ridge regression can be achieved by using the following formula:

$$\begin{aligned}\hat{\xi} &= \arg \min_{\xi} \|\Theta \xi - U_t\|_2^2 + \lambda \|\xi\|_2^2 \\ &= (\Theta^T \Theta + \lambda I)^{-1} \Theta^T U_t.\end{aligned}\quad (9)$$

In order to obtain sparse results, an appropriate threshold tol is introduced to select coefficients. The coefficients that are larger than tol are reserved, while the coefficients that are smaller than tol are omitted. This process will continue with the remaining terms until the number of terms no longer changes.

The detailed procedure of DL-PDE is provided in Algorithm 1.

| Algorithm 1 | | The procedure of DL-PDE |
|----------------------------|--|---|
| | | Design the candidate library $\Phi(u)$ |
| Neural network step | | Design the neural network structure $NN(x, t)$ |
| | | Train the neural network by using the Adam optimizer to minimize the loss function, as shown in Eq. (8). |
| | | Generate meta-data using the trained neural network |
| | | For each meta-data, calculate the derivatives that are required in the candidate library using automatic differentiation. |
| STRidge step | | Split the data into training and testing sets: $\Theta \xrightarrow{80/20 \text{ split}} [\Theta^{train}, \Theta^{test}] \quad U_t \xrightarrow{80/20 \text{ split}} [U_t^{train}, U_t^{test}]$ |
| | | Initialize the parameters and select an appropriate $tol=dtol$ Obtain an estimate of ξ by least squares regression: $\xi_{best} = (\Theta^{train})^{-1} U_t^{train} \quad error_{best} = \ \Theta^{test} \xi_{best} - U_t^{test}\ _2^2 + \eta \ \xi_{best}\ _0$ |
| | | For $iter=1, 2, \dots, tol_iters$: |
| | | Repeat |
| | | Step 1: Use ridge regression to approximate $\hat{\xi}$ $\hat{\xi} = \arg \min_{\xi} \ \Theta \xi - U_t\ _2^2 + \lambda \ \xi\ _2^2$ |
| | | Step 2: Reserve coefficients larger than tol and drop coefficients smaller than tol $\Theta_{new} = \Theta[:, bigcoeffs]$ Use the Θ_{new} with less coefficients to update $\hat{\xi}$ by ridge regression |
| | | until the number of coefficients no longer changes; |
| | | Return $\hat{\xi}$ and calculate the error, $error = \ \Theta^{test} \hat{\xi} - U_t^{test}\ _2^2 + \eta \ \hat{\xi}\ _0$ |
| | | If $error \leq error_{best}$: |
| | | $error_{best} = error$; $\xi_{best} = \hat{\xi}$ $tol = tol + dtol$ |

| | | | |
|--|--|---|--|
| | | | |
| | | Otherwise: | |
| | | $tol = \max([0, tol - 2 \cdot dtol])$ $dtol = \frac{2dtol}{tol_iters - iter}$ $tol = tol + dtol$ | |
| | | Return ξ_{best} | |

3. Results

In this section, we use some classical physical processes described by groundwater flow equation, contaminant transport equation, Burgers equation, and Korteweg–de Vries (KdV) equation to test the performance of the DL-PDE method.

3.1 Learning groundwater flow equation

Firstly, we utilize this method to learn the governing equation of groundwater flow in a saturated confined aquifer. For proof-of-concept, the data are generated through numerical simulation. We consider one dimensional (1-D) flow in a saturated confined aquifer, whose governing equation is as follows:

$$Kh_{xx} = S_s h_t \quad (10)$$

In this case, the conductivity K is supposed to be homogeneous with a value of 1 m/d, and the specific storage S_s is 0.01 m^{-1} . The length of the domain is 1010 m, and the domain is evenly divided into 101 grid blocks of $\Delta x = 10 \text{ m}$. At the initial moment, the hydraulic head is 1 m at the left boundary and 0 m at other locations. There is no source or sink term. We monitor the dynamical flow process from day 0 to day 200 with a measurement interval $\Delta t = 2 \text{ d}$. We utilize a numerical simulation program to generate the data. Here, we assume that the grid block centers and the monitoring locations are coincident. For these data, the number of space observation points $n_x = 101$, the number of temporal observation points $n_t = 100$, and the size of the data $N_d = 10100$.

Since S_s is always very small in the groundwater flow equation, we will pre-process the data prior to proceeding with the algorithm. We use $x^* = \frac{x}{\Delta x}$, $t^* = t$, and $h^* = \Delta x \cdot h$ to replace x , t , and h , respectively, and the equation is converted into:

$$h_t^* = \lambda h_{x^* x^*}^* \quad (11)$$

In this case, $\lambda = 1$. The candidate library is constructed as:

$$\Phi = [1 \quad h_x^* \quad h_{x^*}^* \quad h_{x^*x^*}^* \quad h^*h_x^* \quad h^*h_{x^*}^* \quad h^*h_{x^*x^*}^* \quad h^{*2}h_x^* \quad h^{*2}h_{x^*}^* \quad h^{*2}h_{x^*x^*}^*] \quad (12)$$

The candidate library is a sufficient library with four linear terms and six nonlinear terms. Here, we consider the derivatives up to order three. We use a nine-layer deep neural network with 20 neurons per hidden layer to represent the solution u . Regarding the activation functions, we use $\tanh(x)$. The neural network $NN(x^*, t^*)$ is trained by minimizing the sum of squared errors.

Derivatives are calculated with automatic differentiation. As detailed in section 3.6.2, meta-data and corresponding derivatives that can be generated by the trained neural network are advantageous during the STRidge process. To generate meta-data, we select a section from 40 m to 1050 m, and take a spatial data point every 1 m. Similarly, we choose temporal data points every 0.2 day from day 0 to day 200. For these meta-data, the number of space observation points $n'_x=101$, the number

of temporal observation points $n'_t=1000$, and the size of the data set $N_d=101000$. Its data volume is 10 times the original data volume, which means that we use the trained neural network to generate much more meta-data. This is critical for improving the performance of the sparse regression. Finally, we utilize the derivatives of meta-data to establish a candidate library from Eq. (12), and perform STRidge to obtain the form of the equation and corresponding coefficients.

We now investigate the performance of the DL-PDE method under different data volumes. We train the neural network $NN(x^*, t^*)$ with 2500, 1000, 500, 200 and 100 data, respectively. All of the data are randomly selected. Selected data in the cases of 2500 and 100 data points are shown in Fig. 2. One can see that the selected data are discrete, and their number is small. Then, we use the DL-PDE to find PDE correspondingly. The results are summarized in Table 1.

Table 1. Summary of PDEs founded using DL-PDE for the case of groundwater flow with different data training the neural network.

| Volume of Data | Learned Equation |
|-------------------------------|-----------------------------|
| Correct PDE | $h_t^* = h_{x^*x^*}^*$ |
| 2500 data (24.8% of total) | $h_t^* = 0.992h_{x^*x^*}^*$ |
| 1000 data (9.90% of total) | $h_t^* = 1.018h_{x^*x^*}^*$ |
| 500 data (4.95% of total) | $h_t^* = 0.988h_{x^*x^*}^*$ |
| 200 data (2.48% of total) | $h_t^* = 0.987h_{x^*x^*}^*$ |
| 100 data (1.24% of total) | $h_t^* = 0.731h_{x^*x^*}^*$ |

From Table 1, it is seen that the performance of this algorithm increases as the amount of

training data increases. In the case of small data volume, such as 2% of the original data, the algorithm can still find the form of the equation correctly with relatively accurate coefficients.

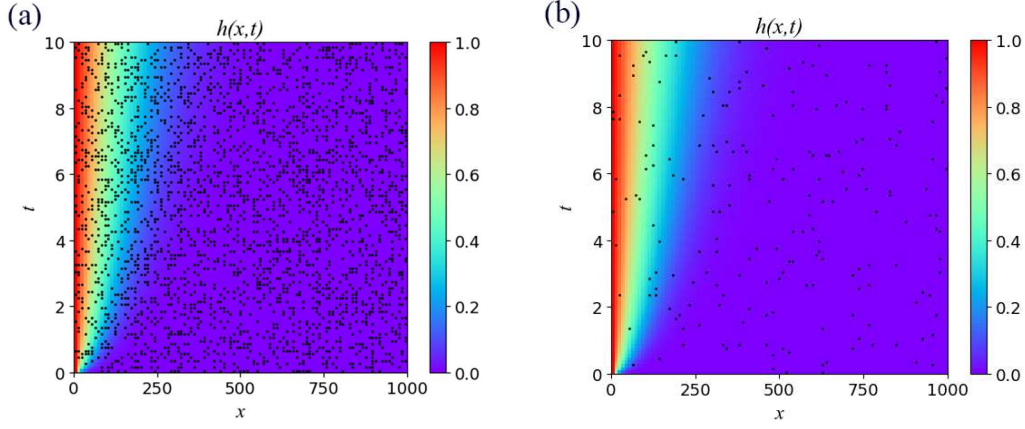


Fig. 2. Randomly selected data from the dataset: 2500 data (a) and 100 data (b). The background represents the solution h in the dataset by heat map, and the black dots are selected data.

Next, we test the performance of DL-PDE when data are noisy. In this work, noise is synthetically added to the data at each monitoring location as follows:

$$u(x, t) = u(x, t) \times (1 + \delta \times e) \quad (13)$$

where δ denotes the noise level; and e denotes the uniform random variable, taking values from -1 to 1 (Chang & Zhang, 2019b). We randomly select 2500 data to train the neural network. Two noise levels, 1% and 5%, are added to the data. The results are summarized in Table 2.

Table 2. Summary of PDEs found using DL-PDE for the case of groundwater flow with noisy data.

| Noise Level | Learned Equation |
|-------------|---------------------------|
| Correct PDE | $h_t^* = h_{x x}^*$ |
| Clean data | $h_t^* = 0.992 h_{x x}^*$ |
| 1% noise | $h_t^* = 0.971 h_{x x}^*$ |
| 5% noise | $h_t^* = 0.906 h_{x x}^*$ |

From Table 2, one can see that the DL-PDE method is robust to noise. For the groundwater flow equation, an earlier work (Chang & Zhang, 2019a) found robust results with 5% noise as well, but with noisy data smoothed and all of the data used. In the present study, although we do not smooth the noisy data, the DL-PDE can still accurately obtain the equation form and corresponding coefficients with only 25% of total data.

3.2 Learning contaminant transport equation

Let us next consider the contaminant transport equation. It is an equation describing the motion of

matter formed by solute or pollutant in fluid. For one-dimensional advection, it is modeled by $-v_x C_x$.

Here, C denotes the solute concentration, and v_x is the average linear fluid velocity. Meanwhile,

the one-dimensional dispersion process is modeled by $D_L C_{xx}$, where D_L represents the longitudinal dispersion coefficient. So, the governing equation reads as:

$$C_t = -v_x C_x + D_L C_{xx} \quad (14)$$

To obtain a set of training data, we simulate the contaminant transport equation Eq. (14) by numerical simulation. v_x and D_L are set to be 1 and 0.25, respectively. The length of the domain is 30 m, and the domain is evenly divided into 120 grid blocks of $\Delta x = 0.25$ m. At the initial moment, there is a source of pollution of $C=12$ at $x=0$, and pollution spreads over time. We monitor the contaminant transport process from day 0 to day 15, and record the solute concentration. The measurement interval is 0.1 d. Similarly, we assume that the centers of grid blocks and the monitoring locations are coincident. For these data, we have $n_x=120$, $n_t=150$, and $N_d=18000$.

We use a nine-layer deep neural network with 20 neurons per hidden layer to represent the solute concentration C . Activation functions are chosen to be $\tanh(x)$. Meta-data and corresponding derivatives are produced by the trained neural network to perform STRidge. To generate meta-data, we select a section from 3 m to 15 m, and take a spatial data point every 0.1 m. Temporal observation points are selected every 0.01 d from day 0 to day 9. For these meta-data, $n'_x=120$, $n'_t=900$, and $N'_d=108000$. The candidate library is established in a similar manner to Eq. (12).

We now test the performance of this method under different data volumes. We train the neural network $NN(x,t)$ with 4000, 2000, 1000, 500, 200 and 100 data, respectively. All of the data are randomly selected. Selected data in the cases of 2000 and 500 data points are shown in Fig. 3. Then, we use the DL-PDE method to find PDE correspondingly. The results are summarized in Table 3. It is seen that, for the contaminant transport equation, we only need a small amount of data to accurately figure out the form of the equation. Moreover, the coefficients of the equation are also relatively accurate. This indicates that this method still works very well in the case of small data volume.

Table 3. Summary of PDEs found using DL-PDE for the case of contaminant transport with different data training the neural network.

| Volume of Data | Learned Equation |
|-------------------------------|---------------------------------|
| Correct PDE | $C_t = -C_x + 0.25C_{xx}$ |
| 4000 data (22.2% of total) | $C_t = -0.999C_x + 0.251C_{xx}$ |

| | |
|---------------------------------------|---------------------------------|
| 2000 data (11.10% of total) | $C_t = -0.998C_x + 0.252C_{xx}$ |
| 1000 data (5.56% of total) | $C_t = -0.999C_x + 0.248C_{xx}$ |
| 500 data (2.78% of total) | $C_t = -1.000C_x + 0.248C_{xx}$ |
| 200 data (1.39% of total) | $C_t = -0.989C_x + 0.246C_{xx}$ |
| 100 data (0.70% of total) | $C_t = -1.005C_x + 0.239C_{xx}$ |

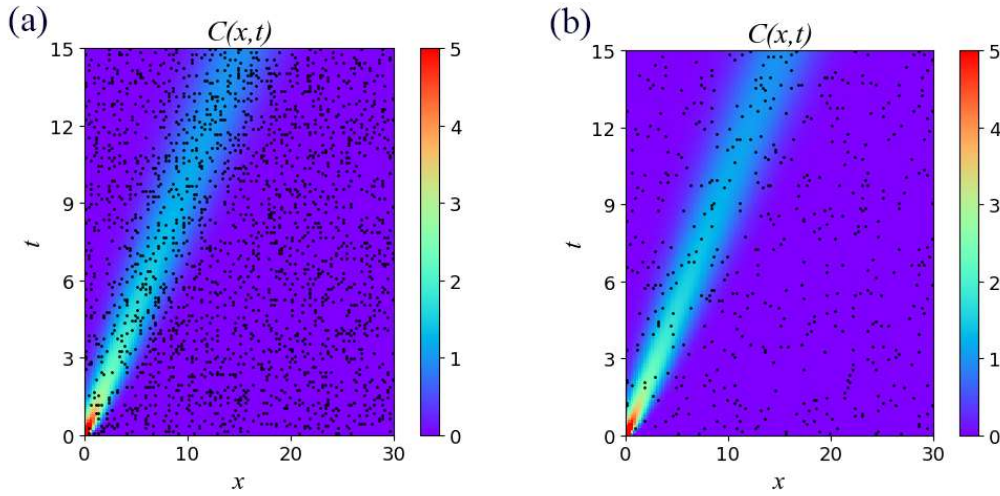


Fig. 3. Randomly selected data from the dataset: 2000 data (a) and 500 data (b). The background represents the solution h in the dataset by heat map, and the black dots are selected data.

We next add noise to the data, randomly select 500 data to train the neural network, and then use the DL-PDE method to find PDE correspondingly. The results are shown in Table 4. For the contaminant transport equation, a previous investigation reported that it is robust to 10% noise, but noisy data are smoothed and all of the data are used (Chang & Zhang, 2019a). In contrast, the DL-PDE method performs very well under noise data conditions, and is robust to 10% noise even with only 2.78% of total data.

Table 4. Summary of PDEs found using DL-PDE for the case of contaminant transport with noisy data.

| Noise Level | Learned Equation |
|--------------------|---------------------------------|
| Correct PDE | $C_t = -C_x + 0.25C_{xx}$ |
| Clean data | $C_t = -1.000C_x + 0.248C_{xx}$ |
| 1% noise | $C_t = -0.996C_x + 0.248C_{xx}$ |
| 5% noise | $C_t = -0.995C_x + 0.247C_{xx}$ |

| | |
|------------------|---------------------------------|
| 10% noise | $C_t = -0.999C_x + 0.239C_{xx}$ |
|------------------|---------------------------------|

3.3 Learning Burgers equation

The Burgers equation is a nonlinear partial differential equation that simulates the propagation and reflection of shock waves. It differs from the Navier-Stokes equations in that it drops the pressure gradient term, which makes it not exhibit turbulent behavior. It arises in various areas of engineering and applied mathematics, including fluid mechanics, nonlinear acoustics, gas dynamics, and traffic flow (Basdevant et al., 1986). One-dimensional Burgers equation can be written as follows:

$$u_t = -uu_x + au_{xx} \quad (15)$$

where a is the diffusion coefficient, and we set $a=0.1$ in this example. Compared with the previous cases, the Burgers equation has a nonlinear term, and thus it is more difficult to find the equation form. We use it to test the performance of the DL-PDE method when finding nonlinear terms.

To obtain a dataset, we utilize conventional spectral methods to simulate the Burgers equation. With an initial condition $u(0, x) = -\sin(\pi x / 8)$, $x \in [-8, 8]$ and periodic boundary conditions, we integrate Eq. (15) from the starting time $t=0$ to the final time $t=10$. This is accomplished with the Chebfun package (Driscoll et al., 2014) with a spectral Fourier discretization with 256 modes and a fourth-order explicit Runge-Kutta temporal integrator with time-step size 10^{-4} (Raissi, 2018). We record the solution every $\Delta t = 0.05$ to obtain 201 observation points in time. For these data, we have $n_x=256$, $n_t=201$, and $N_d=51456$.

The same as the previous examples, a nine-layer deep neural network with 20 neurons per hidden layer is utilized to represent the solution u . Activation functions are $\tanh(x)$. Meta-data and corresponding derivatives are produced by the trained neural network. To generate meta-data, we take spatial data points with $\Delta x = 0.05$ in the domain $x \in [-8, 8)$, and take temporal data points with $\Delta t = 0.05$ from $t=0$ to $t=9$. For these meta-data, $n'_x=320$, $n'_t=180$, and $N'_d=57600$. The candidate library is established as in Eq. (12).

We now assess the performance of the DL-PDE method under small data volumes. Selected data in the cases of 3000 and 1000 data points are shown in Fig. 4. Then, we use the DL-PDE method to find PDE correspondingly. The results are summarized in Table 5. One can see that accurate results can be obtained with small amounts of data, and the performance of DL-PDE is stable even in the case of 2% data.

Table 5. Summary of PDEs found using DL-PDE for the case of the Burgers equation with little data training the neural network.

| Volume of Data | Learned Equation |
|-------------------------------|----------------------------------|
| Correct PDE | $u_t = -uu_x + 0.1u_{xx}$ |
| 3000 data (5.83% of total) | $u_t = -0.996uu_x + 0.099u_{xx}$ |
| 2000 data (3.89% of total) | $u_t = -0.989uu_x + 0.097u_{xx}$ |
| 1000 data (1.94% of total) | $u_t = -0.970uu_x + 0.091u_{xx}$ |

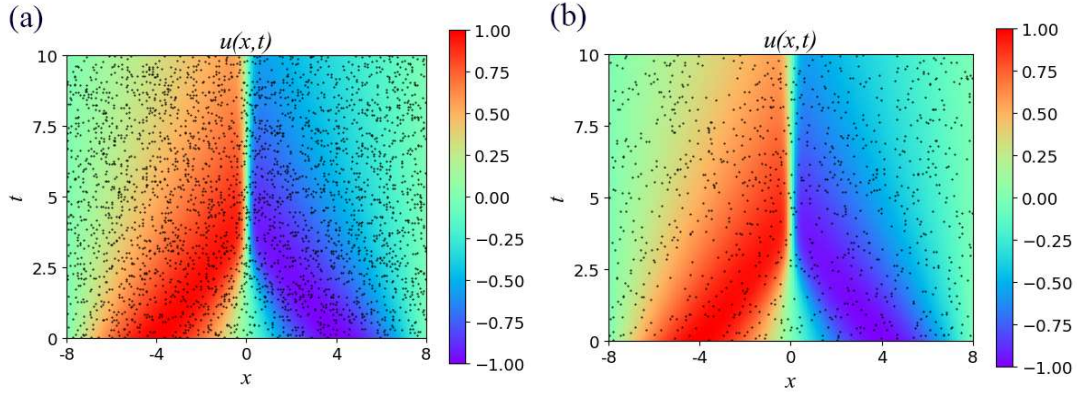


Fig. 4. Randomly selected data from the dataset: 3000 data (a) and 1000 data (b). The background represents the solution h in the dataset by heat map, and the black dots are selected data.

We next add noise to the data, randomly select 3000 data to train the neural network, and then use the DL-PDE method to find PDE correspondingly. The results are shown in Table 6. For the Burgers equation, an earlier work found that it is robust to 1% noise when noisy data are smoothed and all of the data are used (Rudy et al., 2017). In contrast, the DL-PDE is found to be robust to 5% noise even in the case of small data volumes.

Table 6. Summary of PDEs found using DL-PDE for the case of the Burgers equation with noisy data.

| Noise Level | Learned Equation |
|-------------|----------------------------------|
| Correct PDE | $u_t = -uu_x + 0.1u_{xx}$ |
| Clean data | $u_t = -0.996uu_x + 0.099u_{xx}$ |
| 1% noise | $u_t = -0.993uu_x + 0.098u_{xx}$ |
| 5% noise | $u_t = -0.986uu_x + 0.095u_{xx}$ |

3.4 Learning the KdV equation

Finally, we investigate a more complicated equation, the KdV equation. It is a partial differential equation describing one-way motion of shallow water waves. It was discovered by Korteweg and de Vries when studying small-amplitude and long-wave motion in shallow water. Its form is shown in Fig. 5a, and its equation reads as follows:

$$u_t = -uu_x - bu_{xxx} \quad (16)$$

where b is a constant, and we set $b=0.0025$ in this example. Apparently, higher order differential terms appear in the equation, which pose a challenge to the accuracy of calculating derivatives. In previous works, the finite difference method is used to calculate derivatives. However, for higher-order differential terms, the error of the numerical difference method may become non-negligible and even affect the PDE-finding process, leading to finding incorrect equation forms. Therefore, we test the performance of the DL-PDE method in the presence of high-order differential terms.

To obtain a dataset, we utilize conventional spectral methods to simulate the KdV equation. We start with an initial condition $u(0, x) = \cos(\pi x)$, $x \in [-1, 1]$, and assume that boundary conditions are periodic. We integrate Eq. (16) from the starting time $t=0$ to the final time $t=1$. This is done by utilizing the Chebfun package (Driscoll et al., 2014) with a spectral Fourier discretization with 512 modes and a fourth-order explicit Runge-Kutta temporal integrator with time-step size 10^{-6} (Raissi et al., 2019). We record the solution every $\Delta t = 0.005$ to obtain 201 observation points in time. For these data, we have $n_x=512$, $n_t=201$, and $N_d=102912$.

Different from the previous examples, a five-layer deep neural network with 50 neurons per hidden layer is utilized to represent the solution u . Activation functions are changed to $\sin(x)$ in this case since it is found that the sinusoid (i.e., $\sin(x)$) activation function seems to be numerically more stable than $\tanh(x)$ (Raissi, 2018). Meta-data and corresponding derivatives are generated by the trained neural network. To generate meta-data, we take spatial data points with $\Delta x = 0.001$ in the domain $x \in [-0.5, 0.5]$, and take temporal observation points with $\Delta t = 0.005$ from $t=0$ to $t=1$.

For these meta-data, $n'_x=1000$, $n'_t=200$, and $N'_d=200000$. The candidate library is established as in Eq. (12).

We randomly select 25000 data (24.3% of total data) to train the neural network and use the DL-PDE method to find the equation. The selected data are shown in Fig. 5b. The discovered PDEs are given in Table 7. It is seen that this method can still find the correct equation and corresponding coefficients with high accuracy in the presence of high-order differential terms. For the KdV equation, an earlier work found that it is robust to 1% noise when noisy data are smoothed and all of the data are used (Rudy et al., 2017). In contrast, the DL-PDE is robust to 10% noise even with a fraction of data.

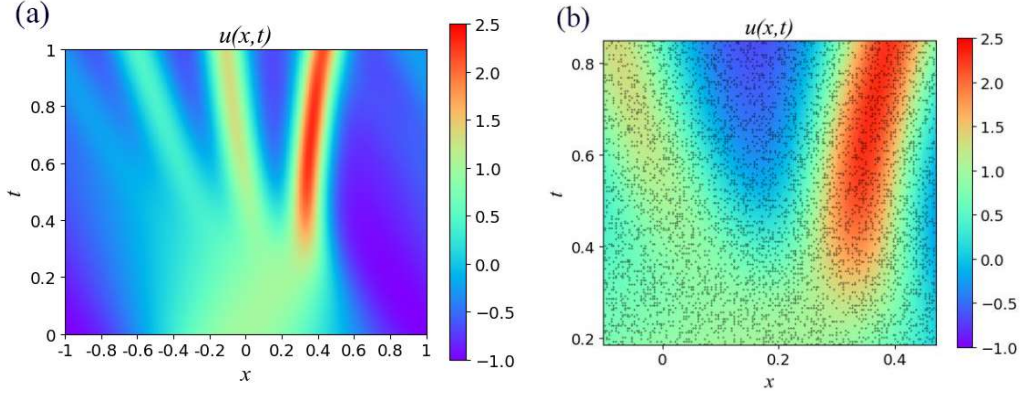


Fig. 5. The solution of the KdV equation in the form of heat map (a) and a portion of the map indicating 25000 data randomly selected from the dataset (b). The background represents the solution u in the dataset by heat map, and the black dots are selected data.

Table 7. Summary of PDE found using DL-PDE for the case of the KdV equation.

| Noise Level | Learned Equation |
|--------------------|-------------------------------------|
| Correct PDE | $u_t = -uu_x - 0.0025u_{xxx}$ |
| Clean data | $u_t = -0.993uu_x - 0.00248u_{xxx}$ |
| 1% noise | $u_t = -0.986uu_x - 0.00247u_{xxx}$ |
| 5% noise | $u_t = -0.968uu_x - 0.00242u_{xxx}$ |
| 10% noise | $u_t = -0.940uu_x - 0.00234u_{xxx}$ |

In addition, as there are high-order differential terms in the KdV equation, more data are needed to enhance the accuracy of the PDE-finding process. In fact, when the amount of data is small, even if the derivatives are automatically calculated by the neural network, the error would be large. Therefore, for the KdV equation, we do not discuss the performance of the DL-PDE with a smaller amount of data.

3.5 Learning PDE in engineering settings

To further scrutinize the performance of the algorithm, we use the DL-PDE method to learn PDE in engineering settings. In previous experiments, observation data points are randomly chosen. However, in actual engineering settings, we may not randomly record data points. In general, there are two ways to record engineering data. The first is to take temporal observations at some limited fixed spatial monitoring locations. For example, in an oil field, a limited number of wells are drilled at fixed locations, from which physical quantities (e.g., production or injection rates) are recorded in time. The second way is to sweep through a space at limited fixed time intervals. For example, an environmental monitoring vehicle passes through an area to measure the concentration of pollutants in a short period of time, or a satellite may cover a certain area to make spatial

observations over a fixed time schedule. Therefore, we may either have a time series of observations at fixed locations x or spatial (continuous or discrete) observations at fixed temporal data points t . In this subsection, we use the DL-PDE to learn PDE in order to test the performance of this algorithm in engineering settings.

We use the contaminant transport equation and the Burgers equation to conduct our experiments. We start with fixed spatial observation locations. For the contaminant transport equation, a total of 12 space observation points is uniformly distributed in the entire domain. For the Burgers equation, a total of 50 space observation points is uniformly placed from $x=-7.9375$ to $x=7.5625$. We select the data at all temporal points at these spatial points as the dataset. Selected data are presented in Fig. 6.

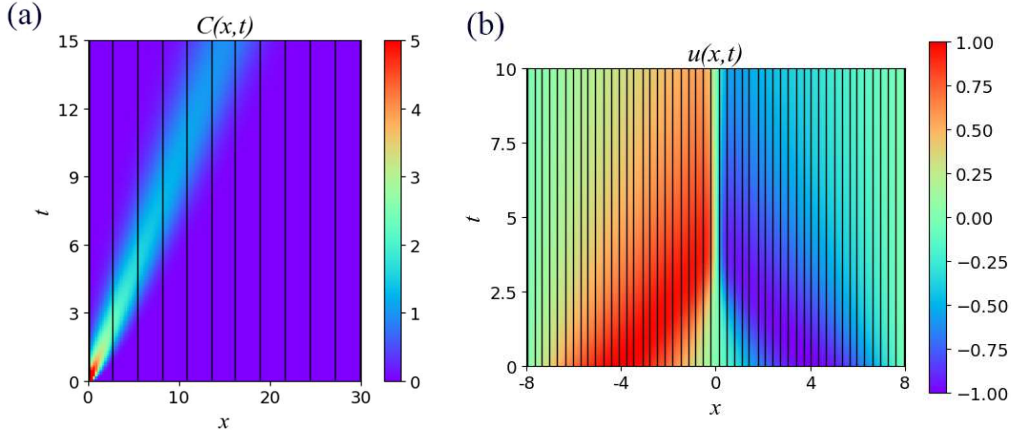


Fig. 6. Generating data from fixed space observation points. Training data are generated from 12 space observation locations in the contaminant transport equation (a) and from 50 space observation locations in the Burgers equation (b). The background represents the solution u in the dataset by heat map, and the black lines are selected data.

A five-layer deep neural network with 50 neurons per hidden layer is utilized to represent the solution u . Activation functions are $\sin(x)$. Meta-data are generated in the same way as in the previous corresponding examples. The results are displayed in Table 8.

Table 8. Summary of PDEs found using DL-PDE for the case of fixed spatial observation data training the neural network.

| Noise Level | Learned Equation (contaminant transport equation) | Learned Equation (Burgers equation) |
|-------------|---|-------------------------------------|
| Correct PDE | $C_t = -C_x + 0.25C_{xx}$ | $u_t = -uu_x + 0.1u_{xx}$ |
| Clean data | $C_t = -1.000C_x + 0.246C_{xx}$ | $u_t = -0.990uu_x + 0.100u_{xx}$ |
| 1% noise | $C_t = -1.000C_x + 0.246C_{xx}$ | $u_t = -0.990uu_x + 0.101u_{xx}$ |
| 5% noise | $C_t = -1.004C_x + 0.246C_{xx}$ | $u_t = -0.973uu_x + 0.097u_{xx}$ |

Next, we fix temporal observation points. For the contaminant transport equation, a total of 15

temporal observation points is uniformly taken in the entire domain. For the Burgers equation, a total of 40 temporal observation points is uniformly taken from $t=0.05$ to $t=9.95$. We select the data at all spatial points at these temporal points as the dataset. Selected data are shown in Fig. 7.

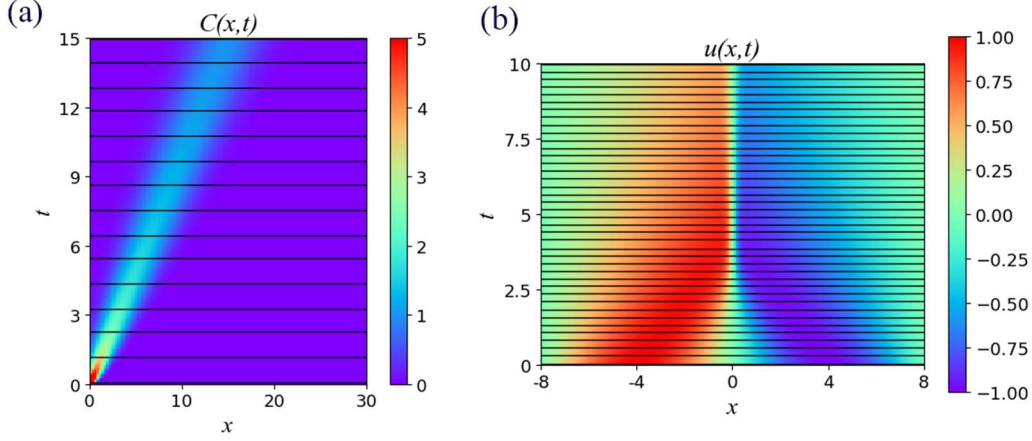


Fig. 7. Generating data from fixed time observation points. Training data are generated from 15 temporal observation points in the contaminant transport equation (a) and from 40 temporal observation points in the Burgers equation (b). The background represents the solution u in the dataset by heat map, and the black lines are selected data.

A five-layer deep neural network with 50 neurons per hidden layer is utilized to represent the solution u . Activation functions are $\sin(x)$. Meta-data are generated in the same way as in the previous corresponding examples. The results are presented in Table 9.

Table 9. Summary of PDEs found using DL-PDE for the case of fixed time observation data training the neural network.

| Noise Level | Learned Equation (contaminant transport equation) | Learned Equation (Burgers equation) |
|-------------|---|-------------------------------------|
| Correct PDE | $C_t = -C_x + 0.25C_{xx}$ | $u_t = -uu_x + 0.1u_{xx}$ |
| Clean data | $C_t = -1.000C_x + 0.250C_{xx}$ | $u_t = -0.997uu_x + 0.100u_{xx}$ |
| 1% noise | $C_t = -1.000C_x + 0.250C_{xx}$ | $u_t = -0.998uu_x + 0.100u_{xx}$ |
| 5% noise | $C_t = -0.996C_x + 0.248C_{xx}$ | $u_t = -0.963uu_x + 0.096u_{xx}$ |

From the two tables above, one can see that, in engineering settings, the DL-PDE method can find the form of the equation and the corresponding coefficients accurately. Extant methods are unsuitable for such problems because they rely on the finite difference method to find the derivatives, but temporal or spatial points here are discrete. It is worth mentioning that we find that, in engineering settings, the DL-PDE is robust to measurement noise. For the case of slight noise (e.g., 1% noise), the DL-PDE performs almost the same as in the case of no noise. Moreover, the DL-PDE behaves well in the case of 5% noise.

3.6 Comparison with other methods

3.6.1 Comparison with direct STRidge

In the DL-PDE, we use a deep neural network to represent physical processes and use the meta-data generated by this neural network to perform sparse regression. Compared with direct STRidge, which calculates the derivatives numerically based on the actual observation data, the DL-PDE relies on deep-learning to come up with the derivatives via automatic differentiation. To further verify the performance of the DL-PDE method, we now compare the performance of the DL-PDE and the direct STRidge.

Firstly, we use these two methods to discover the Burgers equation. The direct STRidge requires the dataset to be on a regular grid, which means that data must be distributed uniformly in space and time. In contrast, the DL-PDE method is more flexible because it can handle discrete data points. In order to compare the performance of these two methods, we use the data points on the same regular grid as the dataset. For this case, we take spatial data points with $\Delta x = 0.0625$ in the domain $x \in [-8, 8)$, and take temporal data points with $\Delta t = 0.05$ from $t=0$ to $t=10$. Consequently, we have $n_x=256$, $n_t=201$, and $N_d=51456$. In order to ensure that the data points are on a regular grid, we reduce the amount of data by selecting one observation point every few observation points in time or space. We use these two methods to discover the Burgers equation with 51456, 12928, and 3264 data, respectively. To obtain 12928 data, we take spatial points with $\Delta x = 0.125$ in the domain $x \in [-8, 8)$ and take temporal points with $\Delta t = 0.1$ from $t=0$ to $t=10$, and we have a subset with $n_x=128$, $n_t=101$, and $N_d=12928$. To obtain 3264 data, we take spatial points with $\Delta x = 0.25$ in the domain $x \in [-8, 8)$ and take temporal points with $\Delta t = 0.2$ from $t=0$ to $t=10$, and we have a subset with $n_x=64$, $n_t=51$, and $N_d=3264$. Selected data are displayed in Fig. 8.

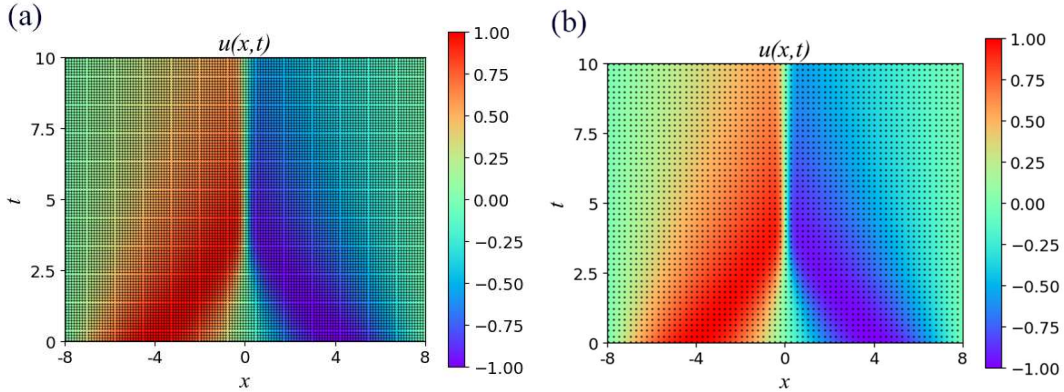


Fig. 8. Selected data from the dataset: 12928 data (a) and 3264 data (b). The background represents the solution u in the dataset by heat map, and the black dots are selected data.

Then, we use DL-PDE and direct STRidge to find the PDE, respectively. Outputs are shown in Table 10. It is seen that, for the Burgers equation, the performances of these two methods are similar in the case of a large amount of data, but when the amount of data is small, the accuracy of direct STRidge is significantly reduced, whereas the DL-PDE method is still relatively more accurate. This shows that the DL-PDE possesses obvious advantages over the direct STRidge for small data volume.

Table 10. Comparison of the performance of the two methods to discover the Burgers equation using different numbers of data.

| | DL-PDE | Direct STRidge |
|--|----------------------------------|----------------------------------|
| Correct PDE | $u_t = -uu_x + 0.1u_{xx}$ | |
| 51456 data (100% of total) | $u_t = -0.998uu_x + 0.099u_{xx}$ | $u_t = -1.001uu_x + 0.102u_{xx}$ |
| 12928 data (25.1% of total) | $u_t = -0.997uu_x + 0.099u_{xx}$ | $u_t = -1.004uu_x + 0.109u_{xx}$ |
| 3264 data (6.34% of total) | $u_t = -0.989uu_x + 0.095u_{xx}$ | $u_t = -1.007uu_x + 0.134u_{xx}$ |

We next compare the performance of these two methods in the presence of noise. In the DL-PDE method, a nine-layer deep neural network with 20 neurons per hidden layer is trained to calculate derivatives. All data are used to train the neural network. In the direct STRidge, a polynomial technique is utilized for smoothing noisy data to obtain stable and relatively accurate derivatives. The procedure is given below (Chang & Zhang, 2019a).

1. For each spatial monitoring point x_0 , smooth the data along t by the procedures below:

A) Select appropriate n^{CH} , N_{CH} , for each t_k , $k=1,2,\dots,n$, generate $1+N_{CH}$ Chebyshev interpolation points t_i^{CH} , $i=1,2,\dots,1+N_{CH}$ on the interval $[t_k - n^{CH} \Delta k, t_k + n^{CH} \Delta k]$.

B) Select appropriate n^{LS} , N_{LS} . For each t_i^{CH} , $i=1,2,\dots,1+N_{CH}$ design an interval $[t_k - n^{LS} \Delta k, t_k + n^{LS} \Delta k]$. Calculate the smoothed value at the Chebyshev interpolation point, $u^{LS}(x_0, t_i^{CH})$ by performing a least squares regression with polynomial up to order N^{LS} using the data inside of the designed interval.

C) Calculate the smoothed value $u^{CH}(x_0, t_k)$ by performing Chebyshev interpolation utilizing the values $u^{LS}(x_0, t_i^{CH})$.

2. Similarly, for each time monitoring point t_0 , smooth the data along x using the same procedures as step 1.
3. Calculate the derivatives with finite difference.
4. Smooth the derivatives with respect to t using the procedures described in step 1, and smooth the derivatives with respect to x using the procedures described in step 2.

Table 11. Comparison of the performance of the two methods to discover the Burgers equation in the presence of noise.

| | DL-PDE | Direct STRidge |
|--------------------|----------------------------------|--|
| Correct PDE | $u_t = -uu_x + 0.1u_{xx}$ | |
| Clean data | $u_t = -0.998uu_x + 0.099u_{xx}$ | $u_t = -1.001uu_x + 0.102u_{xx}$ |
| 1% noise | $u_t = -0.994uu_x + 0.099u_{xx}$ | $u_t = -0.960uu_x + 0.102u_{xx}$ |
| 5% noise | $u_t = -0.992uu_x + 0.098u_{xx}$ | $u_t = -0.824uu_x + 0.117u_{xx} - 0.06u^2u_{xx}$ |

The results are displayed in Table 11. It can be seen that, in the absence of noise, the performance of the two methods is similar, but as the noise level increases, even if the noise has already been smoothed, the accuracy of direct STRidge drops rapidly. Indeed, at the 5% noise level, it is unable to find the correct equation form. In contrast, the performance of DL-PDE is very stable. It is robust to the 5% noise level with high accuracy. This indicates that the DL-PDE is superior to the direct STRidge in the presence of noise.

3.6.2 Comparison with DL-PDE without generating meta-data

In the DL-PDE, meta-data are generated with the trained neural network. When the number of original data is small, it aims to improve the stability of DL-PDE by generating a large number of meta-data to perform sparse regression. To examine this, we compare the performance of the DL-PDE with and without generating meta-data for different cases. In the DL-PDE without generating meta-data, we use the trained neural network to calculate the derivatives of each point on the original dataset without generating meta-data, and then utilize the STRidge to find the PDE. We select the groundwater flow equation and the Burgers equation as our examples, and utilize these two methods to find their corresponding PDEs. Conditions are the same as in previous cases. The results are displayed in Table 12.

Table 12. Comparison of the performance of DL-PDE with or without generating meta-data.

| | DL-PDE with Meta-data | DL-PDE without Meta-data |
|--|----------------------------------|----------------------------------|
| 1. Burgers equation (3000 data used) | | |
| Correct PDE | $u_t = -uu_x + 0.1u_{xx}$ | |
| Clean data | $u_t = -0.996uu_x + 0.099u_{xx}$ | $u_t = -0.993uu_x + 0.099u_{xx}$ |
| 1% noise | $u_t = -0.993uu_x + 0.098u_{xx}$ | $u_t = -0.993uu_x + 0.098u_{xx}$ |
| 5% noise | $u_t = -0.986uu_x + 0.095u_{xx}$ | $u_t = -0.975uu_x + 0.094u_{xx}$ |
| 2. Groundwater flow equation (2500 data used) | | |
| Correct PDE | $h_t^* = h_{x^*x^*}^*$ | |
| Clean data | $h_t^* = 0.992h_{x^*x^*}^*$ | $h_t^* = 1.110h_{x^*x^*}^*$ |
| 1% noise | $h_t^* = 0.971h_{x^*x^*}^*$ | $h_t^* = 0.026h_{x^*x^*}^*$ |
| 5% noise | $h_t^* = 0.906h_{x^*x^*}^*$ | $h_t^* = 0.00024h_{x^*x^*}^*$ |

It is seen from the table above that the stability of DL-PDE can be augmented by generating a large amount of meta-data. When the noise level increases, the DL-PDE with generating meta-data performs better, and the coefficients are more accurate. In the groundwater flow equation, whose original dataset is much smaller than meta-data, when meta-data are not generated, even if the form of the equation can be found, the accuracy of the coefficient is very low in the presence of noise. Hence, it is shown that generating meta-data is critical to improve the stability of the DL-PDE method.

4. Summary and Discussion

In this study, we proposed a novel method, called DL-PDE, combining deep neural network and sparse regression methods such as Lasso, STRidge and sparse Bayesian inference to identify hidden physical process and discover the corresponding governing equations. Compared to extant sparse regression methods for PDE discovery, it is not necessary for the DL-PDE to use numerical differentiation to calculate derivatives, but instead automatic differentiation is used to generate

derivatives via the neural network trained with the observation data. In addition, the use of the meta-data generated by the trained neural network can assist to improve the stability of the sparse regression algorithm, which results in finding the form of the equation and the corresponding coefficients accurately. In this approach, after representing the data accurately with the trained neural network, the underlying physical process can be expressed with a parsimonious model in terms of partial differential equations. Compared to the neural networks alone, interpretability, generalizability, and expandability are substantially improved. In addition, compared to the direct sparse regression methods, problems with limited and noisy data are alleviated, and thus performance is significantly improved.

These assertions are confirmed with demonstrative examples and sensitivity studies. The numerical experiments show that the DL-PDE is robust to data noise. Moreover, without smoothing the noisy data, it can also find the equation form and coefficients accurately. This is mainly because the automatic differentiation of the neural network is less affected by noise and possesses certain robustness to noise. The use of a large number of meta-data generated by trained neural networks also improves the accuracy of the STRidge process.

We have also discussed the performance of DL-PDE in actual engineering settings. Experiments have demonstrated that, in the case of fixed temporal or spatial monitoring points, the DL-PDE method works very well. This indicates that the DL-PDE may be especially suitable for practical applications in which data are usually limited and corrupted with noise.

Finally, we compared the performance of DL-PDE and direct STRidge. Experiments showed that the performance of these two methods is similar when the dataset is large. However, when the number of data is small or the noise level is high, the DL-PDE works better than direct STRidge. In addition, numerical examples confirm that generating meta-data can greatly augment the stability of DL-PDE.

The DL-PDE, at present, is not without limitations. The coefficients in the underlying governing equations are assumed to be constant in space and time. Recent developments in the literature that deal with smoothly varying coefficients (Rudy et al., 2019) or piecewise-constant coefficients (Chang & Zhang, 2019a) may be incorporated in the DL-PDE. However, the general case of spatially (or temporally) randomly distributed coefficients remains a challenge. The recent approach of combining sparse regression with data assimilation (Chang & Zhang, 2019b) that was devised for handling coefficients appearing as a nonlinear function of dependent variables with unknown parameters may prove to be useful for this endeavor, especially after incorporating the deep learning component proposed in this work.

References

- Basdevant, C., Deville, M., Haldenwang, P., Lacroix, J. M., Ouazzani, J., & Peyret, R., et al. (1986). Spectral and finite difference solutions of the burgers equation. *Computers & Fluids*, 14(1), 23-41.
- Baydin, A. G., Pearlmutter, B. A., Radul, A. A., & Siskind, J. M. (2018). Automatic differentiation in machine learning: A survey. *Journal of Machine Learning Research*, 18, 1-43.
- Berg, J., & Nyström, K. (2019). Data-driven discovery of PDEs in complex datasets, *Journal of Computational Physics*, 384, 239-252.

- Boninsegna, L., Nüske, F., & Clementi, C. (2018). Sparse learning of stochastic dynamical equations. *The Journal of Chemical Physics*, 148(24), 241723.
- Brunton, S. L., & Kutz, J. N. (2019). Methods for data-driven multiscale model discovery for materials. *Journal of Physics: Materials*, 2(4), 44002.
- Brunton, S. L., Proctor, J. L., & Kutz, J. N. (2016). Discovering governing equations from data by sparse identification of nonlinear dynamical systems. *Proceedings of the National Academy of Sciences of the United States of America*, 113(15), 3932–3937.
- Champion, K., Lusch, B., Kutz, J. N., & Brunton, S. L. (2019). Data-driven discovery of coordinates and governing equations. *arXiv:1904.02107v2*.
- Chang, H., & Zhang, D. (2019a). Machine learning subsurface flow equations from data, *Computational Geosciences*, DOI: 10.1007/s10596-019-09847-2.
- Chang, H., & Zhang, D. (2019b). Identification of physical processes via combined data-driven and data-assimilation methods, *Journal of Computational Physics*, DOI: 10.1016/j.jcp.2019.05.008, 393: 337-350.
- Chartrand, R. (2011). Numerical differentiation of noisy, nonsmooth data. *ISRN Applied Mathematics*, 2011, 1-11. doi: 10.5402/2011/164564.
- Cullum, J. (1971). Numerical differentiation and regularization. *SIAM Journal on Numerical Analysis*, 8(2), 254-265. doi:10.1137/0708026.
- Cybenko, G. (1989). Approximation by superpositions of a sigmoidal function. *Mathematics of Control Signals & Systems*, 2(4), 303-314.
- Hornik, K., Stinchcombe, M., & White, H. (1989). Multilayer feedforward networks are universal approximators. *Neural Networks*, 2(5), 359-366.
- Jauberteau, F., & Jauberteau, J. L. (2009). Numerical differentiation with noisy signal. *Applied Mathematics and Computation*, 215(6), 2283 - 2297. doi: 10.1016/j.amc.2009.08.042.
- Kaiser, E., Kutz, J. N., & Brunton, S. L. (2018). Sparse identification of nonlinear dynamics for model predictive control in the low-data limit. *Proceedings of the Royal Society A: Mathematical, Physical and Engineering Sciences*, 474(2219), 20180335.
- Kingma, D., & Ba, J. (2014). Adam: A method for stochastic optimization. *arXiv:1412.6980v8*.
- Long, Z., Lu, Y., Ma, X., & Dong, B. (2017). PDE-Net: Learning PDEs from data. *arXiv:1710.09668v2*.
- Lu, L., Meng, X., Mao, Z., & Karniadakis, G. E. (2019). DeepXDE: A deep learning library for solving differential equations. *arXiv:1907.04502v1*.
- Mangan, N. M., Brunton, S. L., Proctor, J. L., & Kutz, J. N. (2016). Inferring biological networks by sparse identification of nonlinear dynamics. *IEEE Transactions on Molecular, Biological and Multi-Scale Communications*, 2(1), 52–63.
- Mangan, N. M., Kutz, J. N., Brunton, S. L., & Proctor, J. L. (2017). Model selection for dynamical systems via sparse regression and information criteria. *Proceedings of the Royal Society A: Mathematical, Physical and Engineering Sciences*, 473(2204), 16. doi:10.1098/rspa.2017.0009.
- Pang, G., Lu, L., & Karniadakis, G. E. (2018). fPINNs: Fractional physics-informed neural networks. *arXiv:1811.08967v1*.
- Quade, M., Abel, M., Kutz, J. N., & Brunton, S. L. (2018). Sparse identification of nonlinear dynamics for rapid model recovery. *Chaos: An Interdisciplinary Journal of Nonlinear Science*, 28(6), 063116.

- Ramos, G., Carrera, J., Gómez, S., Minutti, C., & Camacho, R. (2017). A stable computation of log-derivatives from noisy drawdown data. *Water Resources Research*, 53(9), 7904-7916. doi:10.1002/2017WR020811.
- Raissi, M. (2018). Deep hidden physics models: Deep learning of nonlinear partial differential equations. *Journal of Machine Learning Research*, 19, 1-24.
- Raissi, M. & Karniadakis, G. E. (2018). Hidden physics models: Machine learning of nonlinear partial differential equations. *Journal of Computational Physics*, 357, 125–141.
- Raissi, M., Perdikaris, P., & Karniadakis, G. E. (2017). Machine learning of linear differential equations using Gaussian processes. *Journal of Computational Physics*, 348, 683-693.
- Raissi, M., Perdikaris, P., & Karniadakis, G. E. (2019). Physics-informed neural networks: A deep learning framework for solving forward and inverse problems involving nonlinear partial differential equations. *Journal of Computational Physics*, 378, 686–707.
- Rudy, S., Alla, A., Brunton, S. L., & Kutz, J. N. (2019). Data-driven identification of parametric partial differential equations. *SIAM Journal on Applied Dynamical Systems*, 18(2), 643-660.
- Rudy, S. H., Brunton, S. L., Proctor, J. L., & Kutz, J. N. (2017). Data-driven discovery of partial differential equations. *Science Advances*, 3(4), e1602614. doi:10.1126/sciadv.1602614.
- Schaeffer, H. (2017). Learning partial differential equation via data discovery and sparse optimization. *Proceedings of the Royal Society A: Mathematical, Physical and Engineering Sciences*, 473(2197), 20160446.
- Schaeffer, H., & McCalla, S. G. (2017). Sparse model selection via integral terms. *Physical Review E*, 96(2), 023302.
- Schaeffer, H., Tran, G., & Ward, R. (2017). Learning dynamical systems and bifurcation via group sparsity. *arXiv:1709.01558v1*.
- Schaeffer, H., Tran, G., & Ward, R. (2018). Extracting sparse high-dimensional dynamics from limited data. *SIAM Journal on Applied Mathematics*, 78(6), 3279-3295.
- Yang, L., Zhang, D., & Karniadakis, G. E. (2018). Physics-informed generative adversarial networks for stochastic differential equations. *arXiv:1811.02033v1*.
- Zhang, D., Lu, L., Guo, L., & Karniadakis, G. E. (2019). Quantifying total uncertainty in physics-informed neural networks for solving forward and inverse stochastic problems. *Journal of Computational Physics*, doi:10.1016/j.jcp.2019.07.048.
- Zhang, L., & Schaeffer, H. (2019). On the convergence of the SINDy algorithm. *Multiscale Modeling & Simulation*, 17(3), 948-972.
- Zhang, S., & Lin, G. (2018). Robust data-driven discovery of governing physical laws with error bars. *Proceedings of the Royal Society A: Mathematical, Physical and Engineering Sciences*, 474(2217), 20180305.